J. Phys. Chem. A **2005,** *109,* 6735−6742

Why Are the Ca^{2+} and K^+ Binding Energies of Formaldehyde and Ammonia Reversed with Respect to Their Proton Affinities?

Inés Corral,[†] Otilia Mó,[*,†] Manuel Yáñez,[*,†] and Leo Radom[*,‡]

Departamento de Química, C-9, Universidad Autónoma de Madrid, Cantoblanco, 28049-Madrid, Spain, and School of Chemistry, University of Sydney, Sydney, New South Wales 2006, Australia

Received: March 2, 2005; In Final Form: May 30, 2005

The binding energies (BEs) of alkali metal monocations and alkaline-earth metal dications to a series of small oxygen and nitrogen bases have been evaluated by means of CCSD(T) calculations on B3-LYP optimized structures. These calculations were carried out both using all-electron basis sets, and additionally using an effective-core potential (ECP) to describe the inner electrons of the metal. A theoretical model aiming at analyzing the effects on the binding energy trends of electrostatic, polarization, and covalent contributions, as well as geometry distortion, was employed. From this analysis, we conclude that although the neutral−ion interaction energy for alkali and alkaline-earth metal cations is dominated by electrostatic contributions, in many cases the correct basicity trends are only attained once polarization effects are also included in the model. This is indeed the case when Ca^{2+} and K^+ are bound to ammonia and formaldehyde. Geometry distortions triggered by polarization are also necessary, in some cases, to obtain the correct basicity trends. In addition, in particular for alkaline-earth dications, the energy associated with covalent interactions sometimes dictates the basicity trend. Our observations imply that simple models based on ion−dipole interactions, that are frequently used in the literature to explain affinity trends in ion−molecule reactions, are generally not likely to be reliable.

Introduction

One of the most important achievements of gas-phase ion chemistry has been the determination of so-called intrinsic reactivities, i.e., reactivities that molecules exhibit without the interference of solvent. This has led, in many cases, to a better understanding of chemical bonding. There has been extensive emphasis on the determination of proton affinities and other binding energies.

At the present time, not only have extensive proton affinity scales been established,[1] but basicity scales with respect to several metal monocations (M^+), such as Li^+, Al^+, Na^+, etc., are also known.[2−6] Quite often, at least for homologous series of molecules, the gas-phase M^+ binding energies are linearly correlated with the corresponding gas-phase proton affinities, showing that relative basicities frequently follow similar trends, independent of the reference acid. Some exceptions to this general behavior have also been reported in the literature.[7] One of these exceptions is the enhanced basicity of triazoles, tetrazoles and polyazines toward alkali metal cations.[7,8] This has been attributed to the ability of these metal monocations to give rise to nonclassical bridged structures, in which the cation simultaneously polarizes two (or more) contiguous basic centers. The role of these bridged structures in the interaction of alkali metal cations with small molecules[2,9] and with DNA bases[10,11] has also been well established.

In the past decade, increasing attention has been devoted to the study of complexes involving metal dications, partly because of the development of electrospray experimental techniques that permit the generation of multiply charged species in the gas-phase.[12] This has triggered a number of theoretical studies devoted to the assessment of various theoretical methods for the treatment of doubly charged ions.[13−18] Due to the scarcity of reliable experimental data on binding energies for metal dications, these assessments generally need to be carried out by using high-level ab initio calculations as a reference. This was indeed the case in our recent assessment study for Ca^{2+}, in which we used the W1C and W2C theoretical procedures as a suitable benchmark.[18] One interesting prediction from that work, based on both high-level ab initio and density functional theory procedures, was that the binding energy of Ca^{2+} to formaldehyde is greater than that to ammonia. This contrasts with the well-established observation that the gas-phase basicity of ammonia is larger than that of formaldehyde,[1] and with the fact that the experimental Li^+ binding energies[4] and the G2-calculated Mg^{2+} binding energies[16] follow the same order. A similar basicity inversion was theoretically predicted by Ma et al.[19] when the reference acid is K^+, and confirmed by the calculations carried out in the present study. Also interestingly, it has been found[20] that the binding energy of Na^+ cations to CH_3CHO is greater than to CH_3NH_2, despite the fact that the latter has a much larger proton affinity.

This unusual behavior prompted us to undertake a systematic study of the factors that might be responsible for these basicity inversions. The nonclassical structures that were found in the cases of the azoles and azines mentioned above cannot provide the answer for ammonia and formaldehyde since these are monodentate bases. To broaden the scope of our analysis, we have incorporated in our study several other oxygen and nitrogen bases, namely water, hydrogen cyanide, methanimine, and methylamine, chosen partly on the basis of their electrostatic properties, included in Table 1.[21] HCN was selected because

---

* Corresponding authors. E-mails: otilia.mo@uam.es, manuel.yanez@uam.es, radom@chem.usyd.edu.au.

[†] Universidad Autónoma de Madrid.

[‡] University of Sydney.

10.1021/jp051052j CCC: \$30.25

TABLE 1: Absolute Binding Energies of Metal Mono- and Dications to Selected Bases[a]

base[b]	Li^+			Na^+			K^+			Be^{2+}			Mg^{2+}			Ca^{2+}		
	AE	ECP	lit.	AE	ECP	lit.	AE	ECP	lit.	AE	ECP	lit.	AE	ECP	lit.	AE	ECP	lit.
H_2O 1.85 1.45 691.0	137.0	133.6	140.0[c]	95.6	90.1	94.6 ± 7.5[d] 100[c] 92.5[c]	67.7	61.6	74.9[f] 70.7[g]	592.9	591.2	616.3[h] 583.2[q]	328.2	324.6	336.8[i] 343[j] 328.0[k] 329.6[l]	222.4	204.7	242.6[m] 230[j] 223.5[l]
HCN 2.98 2.59 712.9	146.8	142.3	150[n] 152[o]	106.7	100.1		76.9	70.6	78.4[p]	654.5	652.7		377.0	371.7	376.5[j]	256.1	237.5	
CH_2O 2.33 2.77 712.9	145.1	141.2	151[o] 150[n]	103.8	97.4	95.8[e]	75.7	68.8	77.9[p]	672.9	669.4	623.4[q]	374.6	370.9	375.5[k] 366.5[r]	263.1	240.5	274.7[s]
NH_3 1.47 2.10 853.6	156.4	152.8	161[n] 164[o]	109.1	102.3	107.1[e] 102.2 ± 7[d] 122[s]	74.1	67.0	71 ± 9[g] 79 ± 7[u] 84.1[v]	688.5	687.4	731.8[w]	392.8	386.3	391.7[k] 393.0[l]	255.2	233.0	255.1[l] 266.4[s]
CH_2NH - - 852.9	166.4	162.0	-	117.2	109.9	113.0[e]	81.7	73.9	-	753.5	751.7		431.4	424.2	-	285.0	259.5	
CH_3NH_2 1.31 375 899.0	166.4	162.2	172[o]	115.9	107.9	110.0[e] 134[l] 132.0[x]	78.7	70.1	79.9[g]	760.5	758.6		435.7	427.7	434.2[k]	284.4	256.2	

[a] All binding energies are in kJ mol^{-1}. AE and ECP stand for all-electron and effective-core-potential calculations, respectively. Both sets of values include ZPVE corrections. Unless otherwise noted, values from the literature (lit.) correspond to experimental values. In the absence of such values, theoretical estimates at the level indicated in the corresponding footnote are included. [b] Beneath the name of each base are listed its dipole moment (in D) and its polarizability (in 10^{-24} cm^3) taken from ref 21 and its proton affinity (at 298 K in kJ mol^{-1}) taken from ref 1. [c] Ref 37. [d] Ref 20. [e] Ref 44. [f] Ref 36. [g] Ref 39. [h] MP2/6-311G** level ref 48. [i] MP2/aug-cc-pVTZ level ref 52. [j] CPF/TZ level ref 47. [k] dG2thaw(QCI) level ref 16. [l] G2(QCI) level ref 14. [m] MP2/6-31+G* level ref 52. [n] Ref 38. [o] Ref 41. [p] B3-LYP/6-311+G(3df,2p) level ref 19. [q] CCSD(T)/6-311+G(d,p)//B3-LYP/6-31+G(d) level ref 51. [r] G2 level ref 50. [s] W2C level ref 18. [t] Ref 42. [u] Ref 46. [v] Ref 40. [w] MP2/6-31G(d,p) level ref 49. [x] Ref 43

its dipole moment is slightly greater than that of formaldehyde but its polarizability is slightly smaller. Methanimine was included as the nitrogen analogue of formaldehyde. Finally, methylamine was included because its dipole moment is not very different from that of ammonia, but it has a higher polarizability.

Computational Details

Standard ab initio and density function theory (DFT) calculations were carried out with the Gaussian 98 suite of programs.[22] The geometries of neutral molecules and their complexes with metal mono- and dications were optimized using B3-LYP. The binding energies were then obtained through CCSD(T) (with a (riv,rv) correlation space) single-point energy calculations using the B3-LYP optimized geometries. To estimate the various contributions to the bonding, we have compared all-electron calculations with calculations in which the core electrons of the metal are replaced by an effective-core potential (ECP).

For the all-electron calculations, a 6-311+G(3df,2p) basis set for all atoms was used for geometry optimizations, as well as for the evaluation of the harmonic vibrational frequencies, and hence the zero-point vibrational energy (ZPVE) corrections. The all-electron binding energies were obtained at the CCSD(T)/6-311+G(3df,2p)//B3-LYP/6-311+G(3df,2p) level.

For the ECP calculations, due to the kind of model we propose for our analysis (vide infra), we have chosen a large-core ECP. These pseudopotentials consider the ns and np orbitals, which are unoccupied for the metal cation, as valence orbitals, while all the occupied orbitals are considered as part of the core. For example, for calcium the orbitals below 4s and 4p are treated as the core. This characteristic facilitates the separation of the electrostatic and polarization contribution from the covalent interaction energy, since only these ns and np valence orbitals of the metal will be involved in the charge transfer from the base.

We have chosen the Stuttgart relativistic large-core potential as the ECP[23,24] because it is the only large-core ECP examined here that we found to predict the same basicity ordering as that provided by the all-electron CCSD(T)/6-311+G(3df,2p)//B3-LYP/6-311+G(3df,2p) calculations for the present systems. The other large-core ECPs examined, namely, the SKBJ pseudopotential developed by Stevens and co-workers[25,26] and the LANL1DZ electrostatic core potential,[27] overestimate the binding energy between Ca^{2+} and oxygen bases, and therefore they are not well suited for our analysis.

The Stuttgart relativistic large-core ECP uses, as its default, a double-ζ (DZ) (4s,4p)/[2s,2p] basis set to describe the valence orbitals. However, in a previous study, we found that all-electron DZ basis sets when used with ab initio and DFT methods may not be sufficiently flexible to consistently yield reliable binding energies or even to give the correct basicity ordering for Ca^{2+} dication.[18] In this previous work, we also found that 6-311+G-(3df,2p), a triple-ζ basis which includes diffuse functions as well as polarization functions on both hydrogen and heavier elements, yielded reliable geometries and binding energies. Therefore, to achieve a similar basis set quality when the Stuttgart relativistic large-core ECP is used, we have optimized diffuse and polarization functions for first-, second- and third-row alkali and alkaline-earth elements.

For this purpose, we have followed the optimization scheme used by Glukhovtsev et al.[28] for the construction of G2[ECP] basis sets for bromine and iodine, which yielded results comparable in accuracy to those obtained in all-electron calculations. Extended basis sets have previously been con-

TABLE 2: Variationally Optimized Exponents for Polarization (d,f) and Diffuse (s,p) Functions for Alkali and Alkaline-Earth Elements To Be Used with the Stuttgart Relativistic Large-Core ECP

metal	d	f	s	p
Li	0.1280	0.1605	0.0084	0.0093
Na	0.1093	0.1251	0.0073	0.0286
K	0.1779	0.1012	0.0064	0.0095
Be	0.2820	0.2814	0.0093	0.0196
Mg	0.1888	0.1875	0.0102	0.0130
Ca	0.2287	0.1397	0.0078	0.0077

structed using the same procedure[29,30] for elements such as Sn and Pb for use with different ECPs. Hence, to construct our 6-311+G(3df,2p)-type basis sets for Li, Na, K, Be, Mg,and Ca, we have started by completely uncontracting the original DZ [31,31] set, generating a QZ [1111,1111] basis set. The d function exponents were then optimized through QCISD(T) calculations on the MH and MH_2 B3-LYP/6-311+G(3df,2p) optimized geometries, where M is the alkali or the alkaline-earth metal considered in this work. These QCISD(T) optimizations were carried out with the [1111,1111] sp contraction scheme for the metal and a 311G(p) basis for hydrogen. To create multiple sets of d functions from a single optimized function, we have adopted the usual procedure, in which the new exponents are obtained as multiples $n\alpha_d$ and fractions α_d/n of the single optimized exponent α_d. For first- and second-row elements, $n = 2$ and $n = 4$ are used for splitting into two and three functions,[31,32] while values of $n = 2$ and $n = 3$, respectively, are used for (2d) and (3d) splitting in third-row elements.

With the [1111,1111,1] valence basis set generated in the previous step, the diffuse s and p exponents were optimized independently, at the QCISD(T) level, for the M^- (M = Li, Na and K) and MH^- (M = Be, Mg and Ca) anions, the latter with their B3-LYP/6-311+G(3df,2p) optimized geometries. The set of f polarization functions was then obtained through QCISD(T) calculations combined with the [1111,1111,11] valence basis set for all the alkali and alkaline-earth hydrides. The optimized values for all the exponents of polarization and diffuse functions determined in the present study are shown in Table 2. Thus, for geometry optimizations, at the B3-LYP level, the ECP with a [1111,1111,111,1] plus a diffuse sp set for the metal is combined with a 6-311+G(3df,2p) basis set for the remaining atoms of the system. This basis set for the metals will be referred to as [ECP]6-311+G(3df,2p).

Electrostatic and polarization contributions are known to play a significant role in the interactions between a metal cation and a base.[13,33] For example, for complexes with alkali metal monocations, these electrostatic and polarization interactions are the main contributors to the bonding,[8,13] the covalent effects being rather small. For complexes with metal dications such as Ca^{2+}, electrostatic and polarization effects must be stronger, while covalent interactions are still small. There is an additional binding energy contribution that comes from the geometry distortion that is mainly the result of polarization effects arising from interaction between the neutral base and the cation. Although further geometry distortions associated with covalent interactions exist, they are generally less significant, as we shall show later.

A variety of energy partitioning techniques have been proposed in the literature to estimate the extent of the various contributions to the bonding.[34] In the present paper, we have used a theoretical model that was inspired by the technique used by Horn and Ahlrichs[35] to measure the ionic character of bonds, and the method used by Magnusson[13] to estimate the covalent contributions to the binding energies.

The model that we have employed uses B3-LYP/6-311+G(3df,2p) geometries in conjunction with CCSD(T) single-point energies (other than for the electrostatic energies where B3-LYP/6-311+G(3df,2p) was used) and the following procedures:

(a) The electrostatic interaction energies (elect) were estimated by evaluating the molecular electrostatic potential created by the base in its optimum geometry at the point at which the metal is located in the B3-LYP/6-311+G(3*df*,2*p*) geometry of its complex. Twice this value is used for the dications. It should be noted that, strictly speaking, this model considers the cation as a point charge.

(b) The combination of electrostatic and polarization interactions (elect + pol) was estimated as the interaction energy of the base (again in its optimum geometry) with the metal mono- or dication, as described by the ECP exclusively, i.e., without including the corresponding valence functions for the metal. In this way, only the polarization of the base is taken into account, with no charge transfer from the base to the metal cation being able to take place.

(c) To add the effect on binding energy of the geometry distortion associated with polarization to the electrostatic and polarization contributions (elect + pol + def(pol)), we have optimized the geometry of the complex at the B3-LYP/[ECP]/6-311+G(3df,2p) level, keeping the metal−ligand distance frozen to a value equal to that in its B3-LYP/6-311+G(3df,2p) optimized geometry. The notation [ECP]/6-311+G(3df,2p) indicates that while 6-311+G(3df,2p) is used for the other atoms, the metal is described exclusively by its core potential, i.e., without including valence basis functions. This applies both to the geometry optimizations and to the CCSD(T)/[ECP]/6-311+G(3df,2p) energy calculations.

(d) Covalent contributions were included (elect + pol + def(pol) + cov) by estimating the interaction energy between the base and the mono- or dications at the CCSD(T)/[ECP]6-311+G(3df,2p) level, using the geometry optimized in the previous step but including for the metal not only the ECP, but the corresponding valence basis as well.

(e) The full ECP binding energy was obtained using the same scheme as in step d, but after fully optimizing the geometry of the complex (elect + pol + def(pol) + cov + def(cov)) at the B3-LYP/[ECP]6-311+G(3*df*,2*p*) level. The energy change with respect to step d, obtained through single point CCSD(T)/[ECP]6-311+G(3df,2p) calculations, measures the effect of the geometry distortion caused by the covalent contribution. As we shall show later, this geometry distortion is much less important than the one arising from polarization effects.

(f) The full all-electron binding energy was obtained for comparison using conventional CCSD(T)/6-311+G(3df,2p)//B3-LYP/6-311+G(3df,2p) calculations.

Results and Discussion

The calculated binding energies are compared in Table 1 with available experimental data.[19,20,36−46] Due to the scarcity of experimental values, in particular when dealing with metal dications, we have listed higher level theoretical estimates reported in the literature[14,16,18,47−52] for those cases in which relevant experimental information is not available. In general, our calculated binding energies are in reasonable agreement with the available experimental values and the previous high-level theoretical estimates.

It is worth noting to begin that there is an excellent linear correlation between the calculated all-electron binding energies

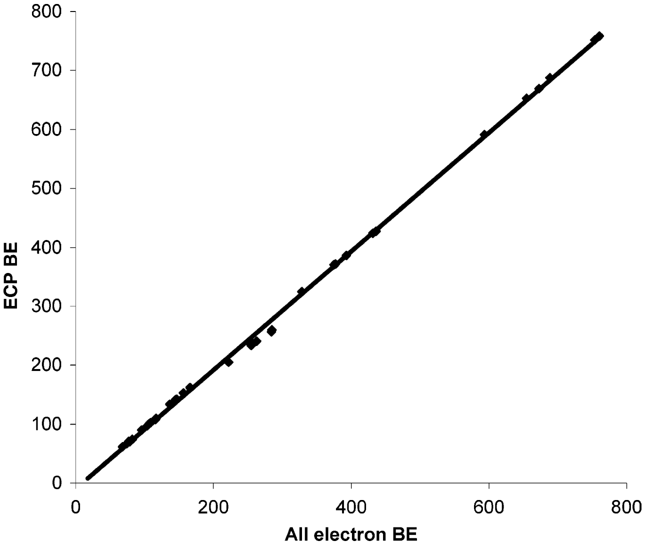

Figure 1. Linear correlation between binding energies (BEs) calculated with all-electron and ECP procedures for alkali and alkaline-earth metal cation complexes with nitrogen and oxygen bases after including ZPVE corrections, leading to BE(ECP) = 1.0072 BE(all-electron) −10.015, with $r^2 = 0.999$.

and those obtained through the use of the ECP approach (see Figure 1). This good correlation lends confidence to the reliability of our estimates of the contributions of the various components to the final BE, obtained using the ECP model described above.

Since we are interested in the trends rather than in the absolute values, we have evaluated the relative contributions of the different components of the total binding energy, taking as a common reference water, which is systematically the least basic of all the molecules under scrutiny in this study. It is worth noting that the relative BE(ECP) and relative BE(all-electron) values follow essentially the same trends, and the relative BEs are very similar in magnitude (see Figure 2). Only for Ca^{2+}, and to a lesser degree for K^+ and Mg^{2+}, are the differences larger because, as expected for these cations, the large-core ECP should be less accurate. For example, it is now well established that the inclusion of "inner-valence" orbitals in the correlation space (as opposed to them being part of the frozen core) is an essential aspect of obtaining reliable results for Ca- and K-containing molecules.[53] Nevertheless, even in these cases the basicity trends obtained in all-electron calculations are correctly reproduced by the ECP approach.

The relative contributions to the binding energies are summarized in Table 3. The first two columns include the electrostatic (elect), and electrostatic + polarization (elect + pol) effects, respectively. Column three adds the geometry distortion effects triggered by polarization (def(pol)). In columns four and five, the covalent interactions (cov) and the resulting geometry distortions (def(cov)) are added to the model. Column six (relative BE(ECP)) includes the ZPVE corrections to yield the best relative ECP binding energies.

It must be noted that small variations in relative values do not necessarily imply small changes in absolute values. For example, covalent effects are expected to be important in Be^{2+} complexes and, indeed, these effects account for 147−177 kJ mol^{-1} of their absolute binding energies. However, as shown in Table 3, the effect of including covalent interactions for the complex between Be^{2+} and HCN, for example, leads to a change of just 3.4 kJ mol^{-1} in the relative binding energy.

To better follow our discussion, it is worth recalling here that the gas-phase proton affinities for the set of molecules under investigation in this study follow the trend: H_2O < HCN ∼ CH_2O < NH_3 ∼ CH_2NH < CH_3NH_2 (see Table 1).[1] The first conspicuous fact from Table 3 is that this pattern is not reproduced for any of the metal cations. For example, while the PAs of HCN and CH_2O are practically equal, their Be^{2+} binding energies differ by about 17 kJ mol^{-1}. Also, as mentioned in the Introduction, ammonia behaves as a stronger base than formaldehyde for H^+, Li^+, Na^+, Be^{2+}, and Mg^{2+}, while the binding energies of K^+ and Ca^{2+} to ammonia are about 2 and 7 kJ mol^{-1}, respectively, lower than those to formaldehyde. It has also been reported in the literature,[20] as another somewhat unexpected result, that NH_3 binds more strongly than H_2O to Li^+ and Na^+, despite water having a larger dipole moment.[3] These findings have been previously explained in terms of the effective position of the dipole of the two systems.[54] However, neutral−cation electrostatic interactions depend not only on the dipole moment of the base, but also on the existence of higher multipoles, and therefore it is desirable to take into account the whole multipole expansion by evaluating the corresponding molecular electrostatic potential. When this is done, the electrostatic interaction of water with mono- and dications is systematically lower than that of ammonia (see first column of Table 3), despite the fact that the dipole moment of water is larger than that of ammonia.

This is also the case in the comparison of HCN and H_2O. Although the dipole moment of HCN is larger than that of water, the electrostatic potential is rather similar for the two molecules, the largest differences being 5.3 and 15.2 kJ mol^{-1} for Li^+ and Be^{2+} complexes, respectively. Polarization effects clearly favor the association to HCN, and this situation remains when geometry distortion effects, covalent contributions and ZPVE corrections are included in the model. Accordingly, HCN is more basic than H_2O, not only in protonation processes but also with any of the reference acids considered in this work.

If HCN is now compared with ammonia, the electrostatic potential is, in all cases, larger for ammonia despite its smaller dipole moment. When polarization effects are included, the BE gap decreases (from 36.0 to 6.5 kJ mol^{-1} for Li^+, from 113.8 to 38.9 kJ mol^{-1} for Be^{2+}, and from 58.0 to 7.2 kJ mol^{-1} for Mg^{2+}) or even changes sign (from 19.8 to −0.9 kJ mol^{-1} for Na^+, from 8.9 to −7.4 kJ mol^{-1} for K^+, and from 34.0 to −10.7 kJ mol^{-1} for Ca^{2+}). The reason the inversion of the BE gap is only observed for Na^+, K^+ and Ca^{2+} can be understood by noting that the electrostatic interaction difference becomes smaller as the metal cation becomes larger, and therefore only in these cases are polarization effects able to counterbalance this difference. The situation does not change significantly when geometry distortion effects are included, although the gap does close a little, and for Na^+ it changes sign. This implies that, if only electrostatic + polarization + geometry distortion effects were playing a role, one should expect, K^+ and Ca^{2+} to bind slightly more strongly to hydrogen cyanide than to ammonia. Quite unexpectedly, this situation is modified for these two cations when covalent effects are added, and both K^+ and Ca^{2+} attach to HCN and NH_3 with almost identical binding energies. Similarly, for Na^+ the inclusion of covalent effects enhances further the interaction with ammonia and its binding energy is larger than that to HCN.

Hence, one important conclusion of this analysis is that, although for alkali and alkaline-earth metal cation complexes the dominant interactions are electrostatic + polarization, in some cases the correct binding energy ordering is only recovered when the geometry distortion and covalent contributions are included in the model. Somewhat similarly, in a study of the

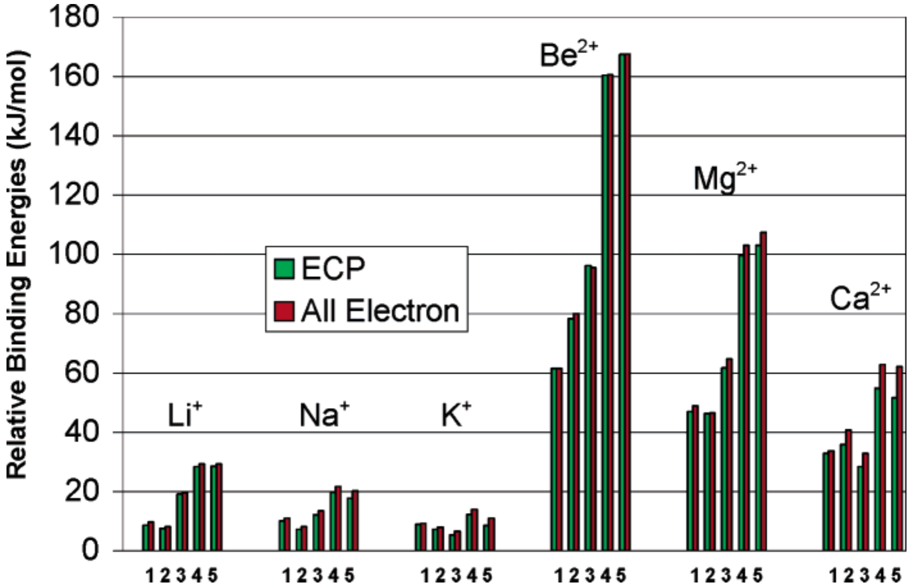

Figure 2. Comparison between all-electron (AE) and effective-core-potential (ECP) binding energies (in kJ mol^{-1}) relative to H_2O. Along the horizontal axis, 1 = HCN, 2 = CH_2O, 3 = NH_3, 4 = CH_2NH, and 5 = CH_3NH_2.

binding of Li^+, Na^+, K^+, Mg^{2+}, and Ca^{2+} to water, ammonia, hydrogen sulfide and phosphine, Magnusson found that covalent effects explain the major departures from electrostatic behavior.[13]

Let us analyze in detail some other illustrative cases where covalent effects and geometry relaxation contributions play an important role in determining the correct basicity trend. Formaldehyde and HCN have almost identical gas-phase proton affinities.[21] However, their binding energies to metal mono- and dications, although generally rather close, show larger differences for Be^{2+} and, to a lesser extent, for Ca^{2+}. As can be seen in Table 3, the electrostatic interactions are always more favorable for HCN than for CH_2O, but the binding energy gap practically disappears (K^+) or even changes sign (Li^+, Na^+, Mg^{2+}, and Ca^{2+}) when polarization and geometry relaxation effects are included. Be^{2+} is the only exception because, in this case, the electrostatic interaction gap is so large that it is not fully counterbalanced by the polarization and geometry distortion contributions. The effect of including covalent interactions is, as expected, rather small for alkali cations but significantly larger for dications, in particular for Be^{2+}. Nevertheless, for Li^+, Na^+, and K^+ the inclusion of covalent interactions changes the trend and now HCN is predicted to bind these ions slightly more strongly than CH_2O, while for the alkaline-earth dications it is the other way around. Changes associated with the geometry distortion triggered by the inclusion of covalent interactions and with the ZPVE are very small, and the final result is that alkali metal cations bind HCN more strongly than CH_2O, while Be^{2+} and Ca^{2+} are predicted to bind CH_2O more strongly than HCN. For Mg^{2+} the two binding energies are rather similar.

Methylamine can be taken as an illustrative example of the significant role that geometry relaxation effects arising from the polarization contribution may play in obtaining the correct basicity order. If geometry relaxation effects coming from the polarization effects are neglected, methanimine is predicted to be a stronger base than methylamine independent of the reference acid (see second column of Table 3), with the only exception being Be^{2+} for which both values are very close. However, methylamine is more easily distorted by cation attachment, leading to larger polarization effects. Accordingly, when geometry relaxation effects are included, the binding energy gap reduces significantly so that methylamine and methanimine are predicted to have rather similar BEs, again with the exception of Be^{2+}, for which the methylamine binding energy is clearly higher. Some interesting basicity inversions are found, with methanimine predicted to bind, Na^+, K^+ and Ca^{2+} more strongly than methylamine, despite the fact that the PA of methylamine is 80 kJ mol^{-1} larger than that of methanimine.[1]

Geometry distortions associated with polarization are also important in obtaining the correct basicity trend in the case of HCN and CH_3NH_2. When only electrostatic + polarization effects are included in the model, Li^+, Na^+, Be^{2+}, and Mg^{2+} bind more strongly to CH_3NH_2 than to HCN, while the opposite behavior is found when the reference acids are the larger cations, K^+ and Ca^{2+}. Geometry distortion effects, which clearly favor methylamine in this case, again cause the binding energy difference to change sign in the case of Ca^{2+}, become slightly smaller for K^+, and increase for the smallest cations Li^+, Na^+, Be^{2+}, and Mg^{2+}. The addition of covalent effects and the geometry distortion contributions associated with them, are also quantitatively significant. For example, for K^+ they are responsible for a change in the sign of the gap (from −4.2 to +1.5 kJ mol^{-1}). For Na^+ and for Ca^{2+}, they are responsible for an increase in the energy gap from 4.8 to 10.2 kJ mol^{-1} and from 9.0 to 20.7 kJ mol^{-1}, respectively, in favor of methylamine.

Geometry distortion contributions to the binding energies induced by covalent effects are found to be generally small (less than 3 kJ mol^{-1} in all cases), and their inclusion does not introduce any significant changes to the basicity trends.

It is also interesting to analyze in detail the effects associated with methyl substitution, in going from ammonia to methylamine. The differences in the electrostatic interactions are generally small (0.1−3.0 kJ mol^{-1}), even when dications are involved. Only for Be^{2+} is this difference large (9.9 kJ mol^{-1}). However, methylamine has a larger polarizability than ammonia, and when polarization and associated geometry relaxation effects are included in the model, the methylamine BEs are systematically larger than those of ammonia. In this case, covalent interactions are also stronger for methylamine than for ammonia, because the methyl inductive effect enhances the electron-donor

TABLE 3: Relative Energy Contributions to the Binding Energies of Metal Mono- and Dications to Bases[a]

	elect	elect + pol	elect + pol + def(pol)	elect + pol + def(pol) + cov	elect + pol + def(pol) + cov + def(cov)	relative BE (ECP) [elect + pol + cov + def(cov) + ZPVE]
				Li^+		
H_2O	0.0	0.0	0.0	0.0	0.0	0.0
HCN	-5.3	5.8	5.4	6.3	6.5	8.7
CH_2O	-14.4	4.8	6.8	6.0	6.2	7.5
NH_3	30.7	12.3	14.4	21.2	21.2	19.1
CH_2NH	26.2	19.9	20.6	28.0	28.6	28.4
CH_3NH_2	30.6	16.4	21.0	29.0	29.2	28.5
				Na^+		
H_2O	0.0	0.0	0.0	0.0	0.0	0.0
HCN	-0.1	6.2	5.7	7.6	7.7	10.0
CH_2O	-6.5	5.0	6.5	5.5	5.6	7.3
NH_3	19.7	5.3	6.9	13.7	13.9	12.2
CH_2NH	17.9	12.4	13.1	19.2	19.5	19.8
CH_3NH_2	17.5	6.7	10.5	17.7	17.9	17.8
				K^+		
H_2O	0.0	0.0	0.0	0.0	0.0	0.0
HCN	1.4	7.5	7.1	6.7	6.7	9.0
CH_2O	-2.1	5.9	6.9	5.4	5.5	7.2
NH_3	10.3	0.1	1.4	6.4	6.5	5.4
CH_2NH	11.1	7.3	8.0	11.3	11.6	12.3
CH_3NH_2	8.2	0.2	2.9	7.9	8.2	8.5
				Be^{2+}		
H_2O	0.0	0.0	0.0	0.0	0.0	0.0
HCN	-15.2	57.8	57.0	60.4	60.8	61.5
CH_2O	-56.4	40.7	50.4	78.4	78.5	78.3
NH_3	98.6	96.7	100.1	99.1	99.0	96.3
CH_2NH	85.4	137.4	141.0	161.2	161.9	160.5
CH_3NH_2	108.5	138.5	155.3	167.1	166.9	167.4
				Mg^{2+}		
H_2O	0.0	0.0	0.0	0.0	0.0	0.0
HCN	-1.1	34.3	33.8	44.9	45.1	47.0
CH_2O	-20.4	34.4	40.5	45.1	45.3	46.3
NH_3	56.9	41.5	45.2	64.4	64.5	61.7
CH_2NH	51.5	71.5	74.1	99.9	100.2	99.6
CH_3NH_2	55.2	64.2	76.7	102.8	103.4	103.1
				Ca^{2+}		
H_2O	0.0	0.0	0.0	0.0	0.0	0.0
HCN	2.0	24.3	23.4	29.8	30.4	32.9
CH_2O	-7.4	21.7	25.8	33.4	34.5	35.8
NH_3	36.0	13.6	18.5	30.2	30.3	28.4
CH_2NH	39.4	33.0	35.1	53.2	54.6	54.8
CH_3NH_2	38.9	23.5	32.4	49.5	51.1	51.5

[a] Relative energies given correspond to the successive inclusion of electrostatic (elect), polarization (pol), geometry deformation arising from polarization (def(pol)), covalent (cov) and geometry relaxation induced by covalent interactions (def(cov)) effects. All values in kJ mol^{-1} relative to the contribution with H_2O as the base.

capacity of methylamine. Hence, when covalent interactions are included, the BE gap increases further, especially for dications.

The inclusion of the ZPVE correction leads to a decrease in the calculated absolute BE due to the presence of an extra bond in the complex, but the effects on the relative BEs are small, as illustrated in Table 3. It is evident, however, that the effect of this correction depends on the strength of the neutral−ion interaction and therefore the absolute values for the ZPVE correction are smaller for K^+ complexes than for Li^+-complexes. However, even for the two extreme cases, namely the Be^{2+}- and K^+-complexes, the inclusion of ZPVE corrections accounts for only 7 kJ mol^{-1}. For example, if a ZPVE correction is not included, the ECP binding energy of methanimine to Be^{2+} is predicted to be 684.6 kJ mol^{-1} higher than its binding energy to K^+. After including the corresponding ZPVE corrections, this gap changes only slightly to 677.8 kJ mol^{-1}. Similarly, the binding energies for K^+ to HCN and NH_3 are almost equal if the ZPVE is not taken into account, and they differ by about 4 kJ mol^{-1} when these corrections are included.

At this point, we address the question of why the ordering of the binding energies of CH_2O and NH_3 to Ca^{2+} and K^+ is the reverse of their binding energies to H^+, Li^+, and Na^+. Although the electrostatic potential is systematically larger for ammonia than for formaldehyde, the inclusion of polarization effects and the geometry distortion associated with them, reduces significantly the energy difference in the case of Li^+, Na^+, Be^{2+}, and Mg^{2+}, and reverses the ordering in the case of K^+ and Ca^{2+}, so that binding to formaldehyde is favored. Covalent effects are larger for ammonia, which is a better electron donor than formaldehyde. Consequently, while the preference for binding to NH_3 increases for Li^+, Na^+, and Mg^{2+} the preference for CH_2O is maintained but decreases for Ca^{2+}, and is reversed to a preference for binding to NH_3 for K^+. Finally, for K^+ and Ca^{2+} cations, the inclusion of covalent geometry distortions and ZPVE corrections increases the preference for binding to CH_2O compared with NH_3. Thus the main contribution to the preference for K^+ and Ca^{2+} to bind to CH_2O rather than to NH_3 appears to stem from the greater polarization effect.

Concluding Remarks

From our analysis we can conclude that a simple electrostatic model cannot reliably explain the trends in metal cation binding energies. Although for alkali and alkaline-earth metal cations, the major part of the neutral−ion interaction energy comes from electrostatic contributions, in many cases the correct basicity trend is only attained once polarization effects are included in the model. This is indeed the case when Ca^{2+} and K^+ are bound to ammonia and formaldehyde. Geometry distortions triggered by polarization are also important to get the correct basicity ordering in some cases (e.g., Ca^{2+} binding with the bases HCN and methylamine), and in others, where the trend is already correct without including geometry distortions, to obtain more reliable energy differences.

In other cases, the energy associated with covalent interactions is important in determining the basicity ordering, or in significantly modulating the values of the binding energy differences. An example of the former situation is provided by the association of HCN and CH_2O with Na^+ or Be^{2+} where, only after including the covalent interactions in the model, is the correct ordering obtained. An example of the latter situation is the interaction of Be^{2+} with formaldehyde and ammonia. After including electrostatic + polarization effects the model correctly predicts ammonia to be more basic than formaldehyde. However, the corresponding energy gap becomes almost three times smaller when covalent interactions are included in the calculation.

In summary, while the correct ordering of basicities for Li^+ can be obtained just through inclusion of electrostatic and polarization contributions, in the case of Ca^{2+} it is necessary to include geometry relaxation contributions, while, quite unexpectedly, for Na^+, K^+, Be^{2+} and Mg^{2+} cations covalent contributions, although small, must be taken into account to achieve the correct ordering. Therefore, simple models based on ion−dipole interactions alone, which are frequently used in the literature to explain affinity trends in ion−molecule reactions, are generally not likely to be reliable.

Acknowledgment. This work has been partially supported by DGI Project No. BQU2003-00894. I.C. gratefully acknowledges an FPU grant from the Ministerio de Educación, Cultura y Deporte of Spain, O.M. thanks the Ministerio of Educación, Cultura y Deporte of Spain for a Visiting Fellowship at the University of Sydney, and L.R. thanks the Australian Research Council for a Discovery Grant. We also gratefully acknowledge generous allocations of computing time from the National Facility of the Australian Partnership for Advanced Computing (APAC), the Australian National University Supercomputing Facility (ANUSF), the Australian Center for Advanced Computing and Communications (AC3), and the Centro de Computación Científica of the Universidad Autónoma de Madrid.

References and Notes

(1) Hunter, E. P.; Lias, S. G. Proton Affinity Evaluation. In *NIST Chemistry Web Book*; *NIST Standard Reference Database Number 69*; National Institute of Standards and Technology: Washington, DC, 2002 (http://webbook.nist.gov) (accessed April 28, 2005).

(2) Hoyau, S.; Norrman, K.; McMahon, T. B.; Ohanessian, G. *J. Am. Chem. Soc.* **1999**, *121*, 8864.

(3) Armentrout, P. B.; Rodgers, M. T. *J. Phys. Chem. A* **2000**, 2238.

(4) Burk, P.; Koppel, I. A.; Koppel, I.; Kurg, R.; Gal, J.-F.; Maria, P.-C.; Herreros, M.; Notario, R.; Abboud, J.-L. M.; Anvia, F.; Taft, R. W. *J. Phys. Chem. A* **2000**, *104*, 2824.

(5) Rodgers, M. T.; Armentrout, P. B. *Mass. Spectrom. Rev.* **2000**, *19*, 215.

(6) Gal, J.-F.; Taft, R. W.; McIver, R. T. *Spectrosc. Int. J.* **1984**, *3*, 96.

(7) Alcamí, M.; Mó, O.; Yáñez, M.; Anvia, F.; Taft, R. W. *J. Phys. Chem.* **1990**, *94*, 4796.

(8) Alcamí, M.; Mó, O.; De Paz, J. J. G.; Yáñez, M. *Theor. Chim. Acta* **1990**, *77*, 1.

(9) McMahon, T. B.; Ohanessian, G. *Chem.*--Eur. J. **2000**, *6*, 2931.

(10) Cerda, B. A.; Wesdemiotis, C. *J. Am. Chem. Soc.* **1996**, *118*, 11884.

(11) Russo, N.; Toscano, M.; Grand, A. *J. Am. Chem. Soc.* **2001**, *123*, 10272.

(12) Jayaweera, P.; Blades, A. T.; Ikonomou, M. G.; Kebarle, P. *J. Am. Chem. Soc.* **1990**, *112*, 2452.

(13) Magnusson, E. *J. Phys. Chem.* **1994**, *98*, 12558.

(14) Petrie, S.; Radom, L. *Int. J. Mass Spectrom.* **1999**, *192*, 173.

(15) Alcamí, M.; González, A. I.; Mó, O.; Yáñez, M. *Chem. Phys. Lett.* **1999**, *307*, 244.

(16) Petrie, S. *J. Phys. Chem. A* **2002**, *106*, 7034.

(17) Merril, G. N.; Webb, S. P.; Bivin, D. B. *J. Phys. Chem. A* **2003**, *107*, 386.

(18) Corral, I.; Mó, O.; Yáñez, M.; Scott, A.; Radom, L. *J. Phys. Chem. A* **2003**, *107*, 10456.

(19) Lau, J. K.-C.; Wong, C. H. S.; Ng, P. S.; Siu, F. M.; Ma, N. L.; Tsang, C. W. *Chem. Eur. J.* **2003**, *9*, 3383.

(20) Armentrout, P. B.; Rodgers, M. T. *J. Phys. Chem. A* **2000**, *104*, 2238.

(21) *NIST Standard Reference Database 101 Release 10*; Computational Chemistry Comparison and Benchmark DataBase; National Institute of Standards and Technology: Washington, DC, 2004 (http://srdata.nist.gov/cccbdb) (accessed April 28, 2005).

(22) Frisch, M. J.; Trucks, G. W.; Schlegel, H. B.; Scuseria, G. E.; Robb, M. A.; Cheeseman, J. R.; Zakrzewski, V. G.; J. A. Montgomery, J.; Stratmann, R. E.; Burant, J. C.; Dapprich, S.; Millam, J. M.; Daniels, A. D.; Kudin, K. N.; Strain, M. C.; Farkas, O.; Tomasi, J.; Barone, V.; Cossi, M.; Cammi, R.; Mennucci, B.; Pomelli, C.; Adamo, C.; Clifford, S.; Ochterski, J.; Petersson, G. A.; Ayala, P. Y.; Cui, Q.; Morokuma, K.; Malick, D. K.; Rabuck, A. D.; Raghavachari, K.; Foresman, J. B.; Cioslowski, J.; Ortiz, J. V.; Stefanov, B. B.; Liu, G.; Liashenko, A.; Piskorz, P.; Komaromi, I.; Gomperts, R.; Martin, R. L.; Fox, D. J.; Keith, T.; Al-Laham, M. A.; Peng, C. Y.; Nanayakkara, A.; Gonzalez, C.; Challacombe, M.; Gill, P. M. W.; Johnson, B.; Chen, W.; Wong, M. W.; Andres, J. L.; Gonzalez, C.; Head-Gordon, M.; Replogle, E. S.; Pople, J. A. *Gaussian 98*, Revision A3; Gaussian, Inc.: Pittsburgh, PA, 1999.

(23) Fuentealba, P.; Preuss, H.; Stoll, H.; Szentpaly, L. V. *Chem. Phys. Lett.* **1982**, *89*, 418.

(24) Fuentealba, P.; Szentpaly, L. V.; Preuss, H.; Stoll, H. *J. Phys. B: At. Mol. Phys.* **1985**, *18*, 1287.

(25) Stevens, W. J.; Basch, H.; Krauss, M. *J. Chem. Phys.* **1984**, *81*, 6026.

(26) Stevens, W. J.; Krauss, M.; Basch, H.; Jasien, P. G. *Can. J. Chem.* **1992**, *70*, 612.

(27) Hay, P. J.; Wadt, W. R. *J. Chem. Phys.* **1985**, *82*, 270.

(28) Glukhovtsev, M. N.; Pross, A.; McGrath, M. P.; Radom, L. *J. Chem. Phys.* **1995**, *103*, 1878.

(29) Gal, J.-F.; Decouzon, M.; Maria, P.-C.; González, A. I.; Mó, O.; Yáñez, M.; El Chaouch, S.; Guillemin, J.-C. *J. Am. Chem. Soc.* **2001**, *123*, 6353.

(30) Salpin, J.-Y.; Tortajada, J.; Alcamí, M.; Mó, O.; Yáñez, M. *Chem. Phys. Lett.* **2004**, 561.

(31) Binkley, J. S.; Pople, J. A. *Int. J. Quantum Chem.* **1975**, *9*, 229.

(32) Frisch, M. J.; Pople, J. A.; Binkley, J. S. *J. Chem. Phys.* **1984**, *80*, 3265.

(33) See for example: (a) Alcamí, M.; Mó, O.; Yáñez, M. *J. Phys. Chem.* **1989**, *93*, 3929. (b) Bauschlicher, C. W.; Langhoff, S. R., Jr.; Partridge, H. In *Organometallic Ion Chemistry*; Freiser, B. S., Ed.; Kluwer Academic Press: Dordrecht, The Netherlands, 1996. (c) Ma, J. C.; Dougherty, D. A. *Chem. Rev.* **1997**, *97*, 1303.

(34) See for example: (a) Kitaura, K.; Morokuma, K. *Int. J. Quantum Chem.* **1976**, *10*, 325. (b) Glendening, E. D.; Streitwieser, A. *J. Chem. Phys.* **1994**, *100*, 2900. (c) Ziegler, T.; Rauk, A. *Theor. Chim.* Acta **1977**, *46*, 1.

(35) Horn, H.; Ahlrichs, R. *J. Am. Chem. Soc.* **1990**, *112*, 2121.

(36) Searles, S. K.; Kebarle, P. *Can. J. Chem.* **1969**, *47*, 2619.

(37) Dzidic, I.; Kebarle, P. *J. Phys. Chem.* **1970**, *74*, 1466.

(38) Staley, R. H.; Beauchamp, J. L. *J. Am. Chem. Soc.* **1975**, *97*, 5920.

(39) Davidson, W. R.; Kebarle, P. *J. Am. Chem. Soc.* **1976**, *98*, 6125.

(40) Castleman, A. W. *Chem. Phys. Lett.* **1978**, *53*, 560.

(41) Woodin, R. L.; Beauchamp, J. L. *J. Am. Chem. Soc.* **1978**, *100*, 501.

(42) Castleman, A. W.; Holland, P. M.; Lindsay, D. M.; Peterson, K. I. *J. Am. Chem. Soc.* **1978**, *100*, 6039.

(43) Guo, B. C.; Purnell, J. W.; Castleman, A. W., Jr. *Chem. Phys. Lett.* **1990**, *168*, 155.

(44) Hoyau, S.; Norrman, K.; McMahon, T. B.; Ohanessian, G. *J. Am. Chem. Soc.* **1999**, *121*, 8864.

(45) Burk, P.; Koppel, I. A.; Koppel, I.; Kurg, R.; Gal, J.-F.; Maria, P.-C.; Herreros, M.; Notario, R.; Abboud, J.-L. M.; Anvia, F.; Taft, R. W. *J. Phys. Chem. A* **2000**, *104*, 2824.

(46) Iceman, C.; Armentrout, P. *Int. J. Mass Spectrom.* **2003**, *222*, 329.

(47) Bauschlicher, C. W., Jr.; Sodupe, M.; Partridge, H. *J. Chem. Phys.* **1992**, *96*, 4453.

(48) Bischof, G.; Silbernagl, A.; Hermansson, K.; Probst, M. *Int. J. Quantum Chem.* **1997**, *65*, 803.

(49) Kerdcharoen, T.; Hannongbua, S. *Chem. Phys. Lett.* **1999**, *310*, 333.

(50) Remko, M.; Rode, B. M. *Chem. Phys. Lett.* **2000**, *316*, 489.

(51) El-Nahas, A. M. *Chem. Phys. Lett.* **2001**, *348*, 483.

(52) Merrill, G. N.; Webb, S. P.; Bivin, D. B. *J. Phys. Chem. A* **2003**, *107*, 386.

(53) See for example: (a) Blaudeau, J.-P.; McGrath, M. P.; Curtiss, L. A.; Radom, L. *J. Chem. Phys.* **1997**, *107*, 5016. (b) Schultz, A.; Smith, B. J.; Radom, L. *J. Phys. Chem. A* **1999**, *103*, 7522. (c) Sullivan, M. B.; Iron, M. A.; Redfern, P. C.; Martin, J. M. L.; Curtiss, L. A.; Radom, L. *J. Phys. Chem. A* **2003**, *107*, 5617.

(54) Langhoff, S. R.; Bauschlicher, C. W. J.; Partridge, H.; Sodupe, M. *J. Phys. Chem.* **1991**, *95*, 10677.